http://dx.doi.org/10.5516/NET.07.2014.027

MICROSTRUCTURE AND MECHANICAL STRENGTH OF SURFACE ODS TREATED ZIRCALOY-4 SHEET USING LASER BEAM SCANNING

HYUN-GIL KIM*, IL-HYUN KIM, YANG-IL JUNG, DONG-JUN PARK, JEONG-YONG PARK, and YANG-HYUN KOO
LWR Fuel Technology Division, KAERI
989-111 Daedeok-daero, Yusenog-gu, Daejeon, 305-353, Republic of Korea
*Corresponding author. E-mail : hgkim@kaeri.re.kr

Received March 10, 2014
Accepted for Publication April 21, 2014

The surface modification of engineering materials by laser beam scanning (LBS) allows the improvement of properties in terms of reduced wear, increased corrosion resistance, and better strength. In this study, the laser beam scan method was applied to produce an oxide dispersion strengthened (ODS) structure on a zirconium metal surface. A recrystallized Zircaloy-4 alloy sheet with a thickness of 2 mm, and Y_2O_3 particles of 10 μm were selected for ODS treatment using LBS. Through the LBS method, the Y_2O_3 particles were dispersed in the Zircaloy-4 sheet surface at a thickness of 0.4 mm, which was about 20% when compared to the initial sheet thickness. The mean size of the dispersive particles was 20 nm, and the yield strength of the ODS treated plate at 500°C was increased more than 65 % when compared to the initial state. This strength increase was caused by dispersive Y_2O_3 particles in the matrix and the martensite transformation of Zircaloy-4 matrix by the LBS.

KEYWORDS : Laser Beam Scanning, ODS, Zircaloy, Strength, Surface Modification

1. INTRODUCTION

Zirconium alloys have been used as a fuel cladding material for a long time because they have good corrosion resistance and irradiation stability in a reactor environment. However, it was recognized that the severe oxidation and creep ballooning behaviors of zirconium alloy cladding tubes at an accident condition of a nuclear reactor have to be considered to improve nuclear plant safety after the Fukushima accident event [1, 2]. The cladding, having an accident tolerant performance, will need to have sufficient oxidation resistance at elevated temperatures to decrease the hydrogen generation needed to prevent hydrogen-related explosions [1], as well as having sufficient strength at elevated temperatures to preserve the fuel rod geometry in order to maintain the core coolability [2]. The coating concept on zirconium alloy cladding is considered to improve the high temperature oxidation resistance [1, 3]. Although the oxidation resistance of zirconium alloy can be improved by the application of coating technology [1, 3], the low strength of zirconium alloy cladding at high temperatures remained as a weak point. This is because the severe deformation of the cladding at increased temperatures is an inherent physical property of zirconium alloy. Thus, the mechanical strength of zirconium-based alloy at high temperature will be increased so as to increase the reactor core coolability.

The oxide dispersion strengthened (ODS) concept is considered to increase the strength of the zirconium-based alloy up to high temperatures. At present, ODS alloys can be applied as structural materials for components in nuclear power plants, since such alloys have a high mechanical strength at high temperatures of up to 700°C [4-6]. This type of alloy is generally manufactured through mechanical alloying from its source metal and Y_2O_3 powders. The mechanical alloyed powders are subjected to the hot isotatic pressing (HIP) or hot extrusion;. The product is then heat treated at the target temperature and time. Thus, the Y_2O_3 particles are dispersed in a metal matrix. The manufacturing processes of ODS alloy are very complex and expensive. In addition, it is necessary that special techniques be used to obtain a uniform dispersion and volume control of Y_2O_3 particles. Another problem is the final product formation such as a tube or sheet since the intermediated-product has a high mechanical strength owing to the dispersion of Y_2O_3 particles. From this, we considered an LBS technique as an alternative method for making the ODS of zirconium-based alloys.

Laser techniques have been applied to the surface modification of ceramics and inter-metallic compounds on a metal base and on ceramic base components. This is to increase the corrosion and wear resistance [7, 8]. A laser heat source can be used for alloying the metal and ceramic materials, as the thermal melting between metal and ceramic is possible [7, 8]. The main advantages and disadvantages of this technology can be summarized as follows:

- Directly applicable to apply to sheet and tube shape components
- Metallurgical damage such as HAZ and severe grain growth is considerably reduced.
- Good control of the alloying element of the treated zone
- Highly reproducible homogeneous zone
- The pores and cracks are suppressed in the treated zone.
- Oxidation can be prevented during the process using inert gas.
- Good control is possible for irregular shaped components.
- Bulk material alloying is limited by the power of the laser source.

Generally, many laser sources such as a pulsed Nd: Yag laser used in SiC coating [7, 8], an excimer pulsed laser used in alumina-13% titania coating [9], and a continuous-wave CO_2 laser used in glass coating [10] are used to obtain good coating properties. However, since this is the first attempt to make the ODS alloy using a laser source, we have to resolve the technical and theoretical issues. In this work, we focused on the Y_2O_3 ODS alloying of a Zircaloy-4 sheet using a continuous-wave diode laser.

Since, it is known that the manufacturing of zirconium alloy is difficult due to the HCP crystal structure of zirconium, the ODS treatment on zirconium alloy is reasonable to the final component such as a tube and sheet. A Zircaloy-4 sheet was used in this work because this alloy has been used as a reference alloy of fuel cladding material, generally. A detailed parametric study such as laser energy, scan speed, Y_2O_3 powder amount, and inert gas flow was carried out to apply the ODS treatment on the surface of a Zircaloy-4 alloy sheet. For the surface ODS treated Zircaloy-4 sheet using LBS, a microstructure analysis using scanning electron microscopy (SEM) and transmission electron microscopy (TEM) was performed, and the strength variation using a tensile tester was also evaluated.

2. EXPERIMENTAL PROCEDURES

2.1 Material

A Zircaloy-4 (Zr-1.5Sn-0.2Fe-0.1Cr in wt.%) alloy sheet was used as a substrate with a dimension of 200 mm x 200 mm x 2 mm, as this material has been used as a fuel cladding tube, spacer grid, and guide thimble tubes of the fuel assembly in a light water reactor. The initial state of the Zircaloy-4 sheet was re-crystallized with a mean grain size of 7 μm. Before the LBS, the substrates were cleaned by alcohol to remove stains or contamination on the surface and then dried. The mean size of the Y_2O_3 powders, which were supplied by Richest Group Ltd., was less than 10 μm; however, their shape and size were very irregular as shown in Fig. 1. Owing to the irregular shape and very small size of the Y_2O_3 powders, the Y_2O_3 powders cannot be supplied using a powder feeder attached to an LBS machine. Thus, these powders were spread onto the Zircaloy-4 sheet in a suspended state with alcohol, and then dried. After drying, the thickness of the Y_2O_3 powder layer was about 25 μm, which was measured using an eddy current tester (ECT).

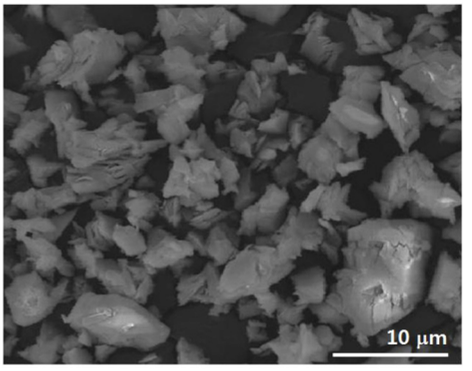

Fig. 1. SEM Observation of the Y_2O_3 Particles before the Laser Beam Scanning (LBS)

2.2 Laser Beam Scanning (LBS)

The surface of the Y_2O_3 spread Zircaloy-4 sheet was scanned by a continuous wave (CW) diode laser with a maximum power of 250 W (PF-1500F model; HBL Co.). The laser scanning parameters to make an ODS layer on the Zircaloy-4 alloy surface were determined from an internal study by controlling the laser power, scan speed, and overlap distance. These parameters are shown in Table 1 and a schematic drawing of ODS treatment is shown in Fig. 2. To prevent oxidation during the LBS, inert gas (Ar) was continuously bellowed onto the melted zone.

2.3 Microstructure Characterization and Tensile Test

The microstructure and composition of an ODS alloying layer for a cross-sectional view have been determined using an optical microscope (OM), SEM with an energy dispersive spectrometer (EDS), and a high resolution (HR)-TEM analysis. The mean diameter and area fraction of the Y_2O_3 particles incorporated in the Zircaloy-4 matrix were calculated from the high magnification of the SEM images. The samples for the TEM observation were prepared using a focused ion beam (FIB).

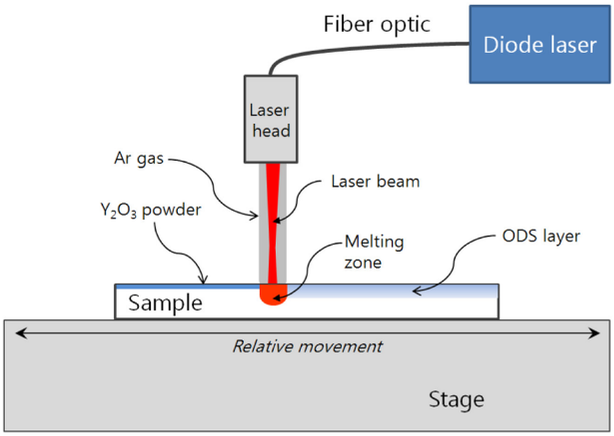

Fig. 2. Schematic Drawing of ODS Treatment in this Work

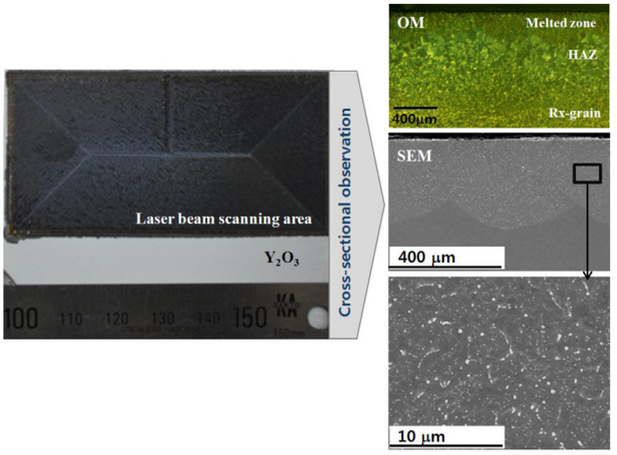

Fig. 3. Surface Appearance after LBS on Zircaloy-4 Sheet and Cross-sectional Observation of ODS Alloying Region

Table 1. Laser Scanning Parameters used to Make ODS Alloying of Zircaloy-4 alloy Sheet

Parameter	Value
Wavelength (nm)	1064
Maximum working power (W)	250
Specific energy (kW/cm^2)	64.1
Scanning speed (mm/s)	3
Overlap (mm)	0.3
Inert gas (Ar) flow (cc/min)	50

A tensile test was performed at room temperature and 500ºC for the ODS alloying sheet through laser scanning methods using an Instron type tensile testing machine. The tensile test was performed following the procedure of ASTM E8 – 82 [11], and the crosshead speed during the tensile test was 1.7 x 10^{-3} s^{-1} for all specimens. Three samples were tested for each condition and very good reproducibility within ± 5% in strength and ductility was confirmed.

3. RESULTS AND DISCUSSION

3.1 Microstructure Characterization of Surface ODS Treated Zircaloy-4 using LBS

A detailed characterization of the oxide dispersion microstructure prepared using the LBS method is very important because it is the first time to make an ODS microstructure of a metal based alloy. Fig. 3 shows the surface appearance after LBS of the Y_2O_3 powder spread on a Zircaloy-4 sheet, and cross-sectional OM and SEM observations of the ODS treated region. In the left part of the figure, different colors in both the LBS area, shown in black, and Y_2O_3 doped area, shown in white, can be observed. In the OM observation, the melted zone with a 0.4 mm layer thickness was shown as having a fine grain structure, and a heat affected zone (HAZ) with a 0.3 mm layer thickness was observed between the melted zone and the recrystallized grain region (initial substrate structure of the Zircaloy-4 sheet). The melted zone was very quickly cooled after the laser beam scan, and therefore, the zone was transformed into a martensite structure. An HAZ was also generally formed near the melting zone during the laser beam scan or laser welding in the metals [12, 13]. From the cross-sectional observation by SEM, it was identified that a wave shape was formed at the substrate and ODS treated layer interface. This wave interface was caused by a repeated LBS line having about a 130 μm beam diameter on the Zircaloy-4 surface, which can be seen in the surface observation. The thickness of an average ODS treated layer of the Zircaloy-4 sheet was about 0.4 mm, and this thickness reached about 20 % of the initial Zircaloy-4 sheet thickness. In a high magnification SEM image, it was observed that the Y_2O_3 particles, which were identified by a SEM-EDS point analysis, were uniformly distributed in the reaction area. From this, the homogeneous mixing area between Zircaloy-4 alloy matrix and Y_2O_3 particles can be obtained in the melting zone. In addition, no voids or cracks in the ODS treated region were observed in this area.

It is known that the melting point of zirconium and Y_2O_3 is 1845ºC [14] and 2439ºC [15], respectively. Although both materials have a high melting point, melting and alloying occur by the application of the laser heat source. Of course, it was reported that SiC and SiO_2 powder mixing can be possible using a Nd:YAG pulsed laser [7], and alumina-13% titnia coating was obtained using an eximer laser [9]. Thus, material with a very high melt-

ing temperature should be melted and alloyed using a laser energy source. However, the threshold energy used to melt the material is dependent on the material types. During the laser treatment, the important technical point in this work is the control of the energy density, scan speed, inert gas flow, and cooling rate. When compared to the Y_2O_3 particle size between initial powders less than 10 μm, as shown in Fig. 1, and the incorporated particles, as shown in Fig. 3, the size of the initial Y_2O_3 particles is considerably decreased after the alloying treatment. A decrease of the Y_2O_3 particle size compared to the initial state was caused by the surface vaporization of Y_2O_3 particles during laser beam heating. The particle size decrease can be identified as a parameter study during the LBS for the Y_2O_3 particles, which were spread on the glass. After the LBS on the Y_2O_3 particles, the size of the particles was significantly decreased by the surface vaporization phenomenon caused by a laser heat source.

Fig. 4 shows the HR-TEM analysis results of the LBS region with the Y_2O_3 particles to evaluate the ODS structure in the zirconium alloy matrix. In the overall appearance from the TEM observation, a plate martensite structure with many dislocations was formed in the LBS region. In the upper images, the Y_2O_3 particles were not clearly identified, such as the SEM observation image, shown in Fig. 3. However, the particle distribution can be analyzed from the EDS mapping profile of yttrium (Ka), and the distribution behavior of the Y_2O_3 particles which can be clearly recognized from the EDS mapping results for the yttrium. The oxide particles formed in the Zircaloy-4 matrix were identified as a Y_2O_3 phase having a cubic structure from the lattice and composition analyses.

To identify the Y_2O_3 particle size and area fraction in the ODS alloying layer, the particle frequency was calculated based on highly magnified SEM and TEM images, as shown in Figs. 3 and 4. The size distribution of the Y_2O_3 particles was divided into two groups between a small size group of about 15 nm and a large size group of about 125 nm. The number density of the small size group is much higher when compared to the large size group. The volume density was increased at the Zircaloy-4 sheet surface, and was gradually decreased when the depth was increased from the surface. This is related to the difference in phase density between Y_2O_3 particles and zirconium metal, because the density of the zirconium matrix is higher than that of Y_2O_3 particles. In the case of the ODS ferritic steel, which was fabricated through mechanical alloying and hot extrusion and annealing procedures, the mean particle size was shown to be 10 nm [16]. Although the matrix composition and manufacturing process between our work and Zhang's work [16] were very different, the fine oxide particles in the matrix can be obtained from both works. When compared to the previous manufacturing process used to make ODS alloy [6, 16], the oxide particle size formed in the matrix was somewhat increased using a laser beaming scanning method. However, it is known that the laser scanning method is very simple and quick for making ODS alloy, as this process is directly applied to the fabricated sheet component. Although some problems such as a control of the particle size and the ODS alloying depth remained in this study, the surface ODS alloyed Zircaloy-4 sheet can be successfully manufactured using the LBS method with oxide powders.

3.2 Tensile Strength Behavior of Surface ODS Al Loyed Zircaloy-4 Sheet

The aim of conventional ODS alloy is to increase the mechanical strength up to the very high temperature of the metal-based alloys. An evaluation of the strength of this alloy is necessary because this is the first time to make ODS Zircaloy-4 using the LBS method. Since the ODS alloyed layer of a Zircaloy-4 sheet is about 0.4 mm, the specimen preparation and test for the only ODS

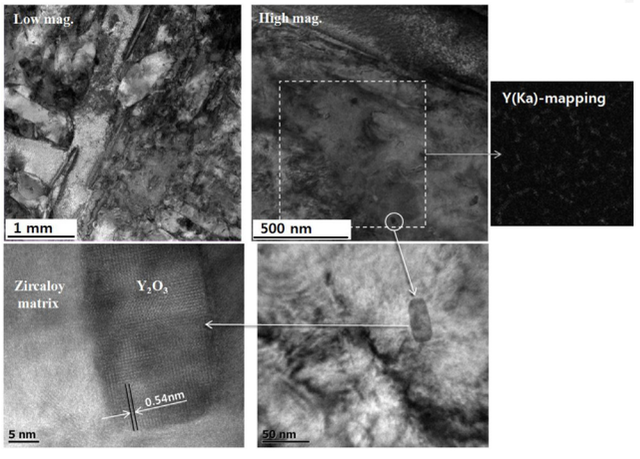

Fig. 4. TEM Analysis of the Y_2O_3 Particles Incorporated in the Zircaloy-4 Matrix

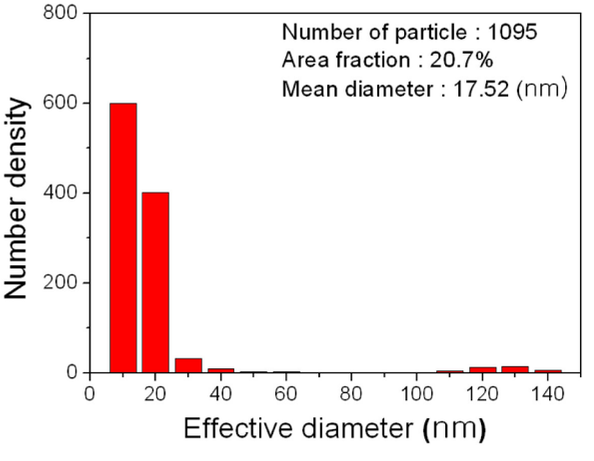

Fig. 5. Size Distribution and Mean Diameter of the Y_2O_3 Particles Incorporated in the Zircaloy-4 Matrix

alloyed layer are very difficult. In this work, the tensile specimens of a dog-born type were prepared from a ODS treated Zircaloy-4 sheet of 2 mm thickness. Thus, the fraction of ODS layer thickness of the tensile specimens was 20%.

Before the tensile tests, it is necessary to consider the mechanical hardening mechanism by LBS, since the strength of metal-based materials can be increased by the martensitic phase transformation and the oxide particle dispersion in the matrix after LBS. Because a martensite structure can be formed by the quick cooling rate from high temperature to room temperature in the zirconium alloys [17, 18], a strength increase is caused by the formation of a martensite structure on the Zircaloy-4 sheet surface by the laser beam treatment. In addition, it is thought that a strength increase resulted from the dispersion of Y_2O_3 oxide particles in the ODS alloyed layer on the Zircaloy-4 sheet surface by the laser beam treatment. Thus, three types of tensile test specimens were prepared to separately evaluate for the three conditions among the initial Zircaloy-4 sheet, surface LBS, and surface LBS with Y_2O_3 oxide powders. To the best of our knowledge, the strength data of the ODS Zircaloy-4 cannot be found, and thus we showed only our data regarding the strength of a partially ODS alloyed Zircaloy-4 sheet, which was produced by the LBS method.

Fig. 6 shows the engineering stress-strain curves of three types of prepared samples consisting of the initial state Zircaloy-4 sheet (marked as initial sheet), surface laser beam scanned Zircaloy-4 sheet (marked as surface LBS), and surface laser beam scanned Zircaloy-4 sheet with Y_2O_3 oxide powders (marked as surface LBS with Y_2O_3 powder). The strength and ductility variations with the prepared samples were clearly shown in both the room temperature and 500°C tests. The tensile tested results, which were averaged from the three tests, are summarized in Table 2. At the room temperature test, the yield strength (YS) and ultimate tensile strength (UTS) were gradually increased by the surface LBS condition to the surface LBS with Y_2O_3 powder condition when compared to the initial state of the Zircaloy-4 sheet. However, the strain elongation behavior of the three tested samples was inversed when compared with the values of YS and UTS. In the 500°C test, the YS and UTS results

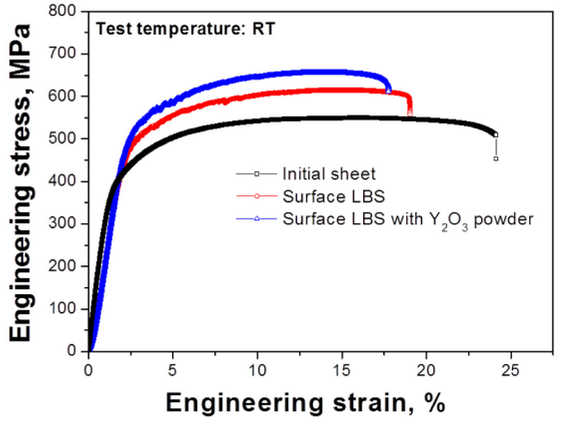

(a) RT test

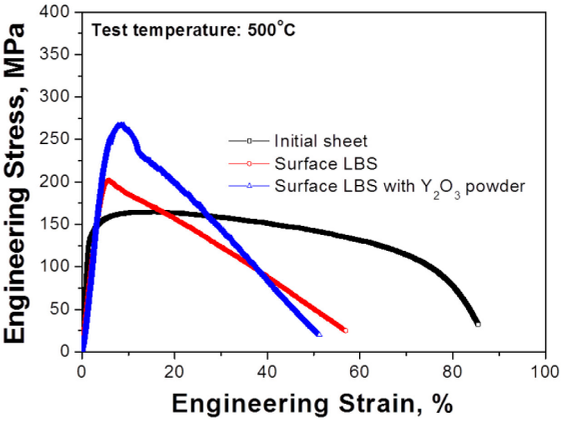

(b) 500°C test

Fig. 6. Engineering Stress-strain Curves of the Different Surface Treated Zircaloy-4 Sheet Samples Tested at RT (a) and 500°C (b)

Table 2. Summary of the Tensile Test Results for the Initial Zircaloy-4 Sheet and the LBS as well as the LBS with Y_2O_3 Powders on the Zircaloy-4 Sheet Surface

Condition		YS (Yield Strength, MPa)	UTS (Ultimate Tensile Strength, MPa)	Ductility (Total Elongation, %)
Initial sheet	RT	423	550	24
	500°C	132	164	85
Surface LBS	RT	489	615	19
	500°C	178	202	58
Surface LBS with Y_2O_3 powder	RT	541	656	17
	500°C	225	266	52

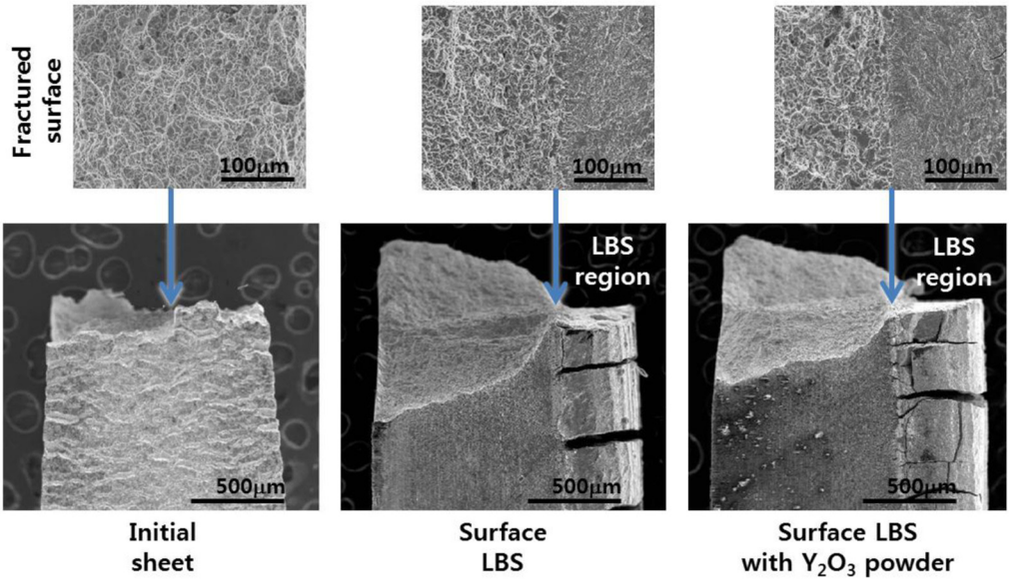

(a) RT test

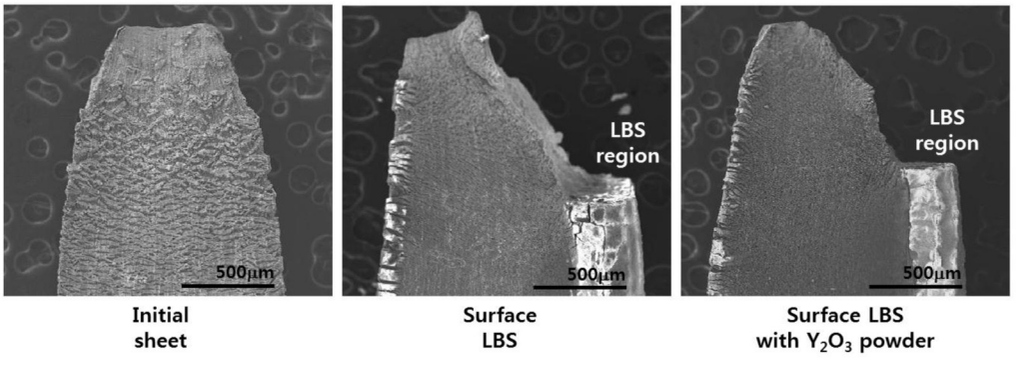

(b) 500°C test

Fig. 7. SEM Observation at the Fractured Region of the Tensile Tested Samples at RT (a) and 500°C (b)

were gradually increased by the surface LBS condition as well as surface LBS with Y_2O_3 powder condition when compared to the initial state of the Zircaloy-4 sheet. In particular, the strength result was considerably improved by the surface LBS treatment with oxide powder. The uniform elongation region of three sample types at 500°C test was very limited when compared to the room temperature test. In addition, the strain elongation of the LBS-treated surface and LBS-treated surface with oxide powder samples was sharply dropped after the highest stress.

Fig. 7 shows the SEM micrographs for the fractured region of the tested samples at both room temperature and 500°C. The fractured shape and dimple morphology was changed by the surface treatment using LBS. After the room temperature test, many small cracks were observed on the initial Zircaloy-4 sheet surface. The surface crack formation at the fractured region in zirconium alloys was caused by the dislocation pile-up to the oriented slip plane of HCP zirconium during the tensile test [19]. The dimple size of initial Zircaloy-4 was higher than those of the other two samples, whereas, the LBS region of the two types of surface LBS-treated samples failed due to a large crack formation, and the dimple size was considerably decreased at the LBS-treated region. From the fractography, the material characteristics of high strength and low ductility can be expected from the LBS treatment. After the 500°C test, the fractured behavior was basically similar to the room temperature test results. However, the elongation of the necking area was increased in all samples, and the frequency of the large crack formation in the LBS region was decreased when compared to the room temperature test. From these mi-

crographs, it was thought that the crack propagation of the surface LBS-treated Zircaloy-4 sheet progressed after the initial cracking of the LBS region, because the ductility of the LBS-treated region was much lower than that of the Zircaloy-4 sheet substrate. Although large cracks were formed in the LBS region, the surface treated layer by LBS was not spalled after the tensile test at both room temperature and 500ºC. Thus, it is known that the interface adhesion property between the Zircaloy-4 matrix and LBS-treated layer is very stable.

When compared to the YS of the initial state Zircaloy-4 sheet, the YS after surface LBS-treated sheet was increased more than 15% at room temperature and 30% at 500ºC, and the YS after surface LBS-treated sheet with Y_2O_3 powder was increased more than 25% at room temperature and 65% at 500ºC, although the LBS-treated layer was 20% for the specimen thickness. It is thought that this strength variation was caused by the microstructural changes such as the formation of martensite structure and the Y_2O_3 particle dispersion in the matrix and by LBS treatment. The martensite structure formation and the Y_2O_3 particle dispersion were clearly confirmed by the TEM microscopic observation for the melted zone as shown in Fig. 4 after the LBS treatment with Y_2O_3 powder. After a comparison of the strength data, as shown in Fig. 6 (a) and (b), it is known that the dispersive Y_2O_3 particles in the martensite matrix were affected by the improvement of the mechanical strength of the Zircaloy-4 alloy, since the surface LBS condition with oxide powder showed higher strength than the surface LBS condition.

An excessive decrease of ductile elongation during the 500ºC tensile test was observed in the surface LBS-treated samples, as shown in Fig. 6 (b). This phenomenon can be thought to be from excess engineering stress, which was much higher than the UTS of the initial Zircaloy-4 sheet, applied to the surface LBS-treated samples during the tensile test. Thus, the Zircaloy-4 matrix cannot resist excess engineering stress after the fracture of the surface LBS-treated layer. This can be recognized from the fractured region of the tested samples at 500ºC, as shown in Fig. 7 (b), because the severely deformed Zircaloy-4 part having a corn shape was observed at the non LBS-treated region.

After a comparison of the strength data, as shown in Fig. 6 (a) and (b), it is evidence that the dispersed Y_2O_3 particles in the martensite matrix improve the mechanical strength of a Zircaloy-4 sheet can be increased by the microstructural changes such as martensite phase formation and Y_2O_3 particle dispersion. From this, it was known that the surface of an ODS Zircaloy-4 sheet can be obtained by the surface LBS treatment with oxide powders, although this treatment cannot obtain the full thickness of an ODS alloy in this stage. This ODS alloying technique can be directly applied to previously manufactured components such as Zirconium alloy claddings, guide tubes, and spacer grids to increase the strength up to high temperatures. Thus, the reactor core coolibility, which was decreased by the strength improvement at high temperature, could be increased by using the ODS alloyed zirconium-based alloy.

4. CONCLUSIONS

Y_2O_3 particles can be successfully dispersed in a Zircaloy-4 sheet surface using an LBS method. Sub-micron Y_2O_3 particles were uniformly distributed in a laser ODS alloyed layer without voids or cracks. The size distribution of the Y_2O_3 particles formed on Zircaloy matrix was divided into two groups consisting of a small-size group of about 15 nm (major) and a large-size group of about 125 nm (minor) for the 0.4 mm thickness layer. From the tensile test at 500ºC, the strength of laser ODS alloying on the Zircaloy-4 sheet was increased more than 65% when compared to the initial state of the sheet, although the ODS alloyed layer was 20% of the specimen thickness. This strength increase was caused by the dispersive Y_2O_3 particles and martensite formation on the Zircaloy-4 sheet using an LBS method. This technology showed a good opportunity to increase the strength without major changes in the substrates of zirconium-based alloys.

ACKNOWLEDGEMENTS

This work was supported by the National Research Foundation of Korea (NRF) grant funded by the Korean government (MSIP) (No. 2012M2A8A5000702).

REFERENCES

[1] H.G. Kim, I.H. Kim, Y.I. Jung, D.J. Park, J.Y. Park, Y.H. Koo, HIGH-TEMPERATURE OXIDATION BEHAVIOR OF CR-COATED ZIRCONIUM ALLOY, TopFuel 2013, Charlotte, North Carolina, September 15-19, 2013, p. 843.

[2] B. Cheng, Y.J. Kim, P. Chou, J. Deshon, DEVELOPMENT OF Mo-ALLOY FOR LWR FUEL CLADDING TO ENHANCE FUEL TOLERANCE TO SEVERE ACCIDENTS, TopFuel 2013, Charlotte, North Carolina, September 15-19, 2013, p. 852.

[3] I. I-.Trujillo, M. Leflem, J-.C. Brachet, M. Lesaux, D. Hamon, S. Muller, V. Vandenberghe, M. Tupin, E. Papin, E. Monsifrot, A. Billard, and F. Schuster, ASSESSMENT AT CEA OF COATED NUCLEAR FUEL CLADDING FOR LWRS WITH INCREASED MARGINS IN LOCA AND BEYOND LOCA CONDITIONS, TopFuel 2013, Charlotte, North Carolina, September 15-19, 2013, p. 860.

[4] J.S. Benjamin, Metall. Trans. 1 (1970) pp. 2943-2951.

[5] S. Ukai, T. Nishida, H. Okada, M. Fujiwara, J. Nucl. Sci. Technol. 34 (1997) pp. 256-263.

[6] C. Cayron, E. Rath, I. Chu, S. Launois, J. Nucl. Mater. 335 (2004) pp. 83-102.

[7] F. Lusquiños, J. Pou, F. Quintero, M. Pérez-Amor, Surface & Coatings Technology, 202 (2008) pp. 1588-1593.

[8] R. Anandkumar, A. Almeida, R. Colaço, R. Vilar, V. Ocelik, J.Th.M.De. Hosson, Surface & Coatings Technology, 201 (2007) pp. 9497-9505.

[9] A. Ibrahim, H. Salem, S. Sedky, Surface & Coatings Technology, 203 (2009) pp. 3579-3589.
[10] J. Yu, W. We, M. Wang, Surface & Coatings Technology, 72 (1995) pp. 112-119.
[11] ASTM E8 – 82; Standard methods of tension testing of metallic materials
[12] Y. Huang, Optics & Laser Tech. 43 (2011) p. 935.
[13] C. Kim, M.J. Kang, Y.D. Park, Procedia Eng. 10 (2011) p. 2226.
[14] D.K. Deardorff, E.T. Hayes, Trans. Am. Inst. Min. Engers 206 (1956) p. 506.
[15] M. Foex, High Temp.-High Press. 9 (1977) p. 269.
[16] C.H. Zhang, A. Kimura, R. Kasada, J. jand, H. Kishimoto, Y.T. Yang, J. Nucl. Mater. 417 (2011) p. 221.
[17] R.A. Holt, J. Nucl. Mater. 35 (1970) p. 322.
[18] H.G. Kim, J.H. Baek, S.D. Kim, Y.H. Jeong, J. Nucl. Mater. 372 (2008) p. 304.
[19] H.G. Kim, I.H. Kim, J.Y. Park, Y.H. Koo, Nucl. Eng. & Tech. 45(4) (2013) p. 505.